

PROCEEDINGS OF SPIE

SPIDigitalLibrary.org/conference-proceedings-of-spie

Computational method for optimizing segmented nonimaging concentrators

Hoffman, Christine, Ilan, Boaz

Christine Hoffman, Boaz Ilan, "Computational method for optimizing segmented nonimaging concentrators," Proc. SPIE 11495, Nonimaging Optics: Efficient Design for Illumination and Solar Concentration XVII, 1149508 (20 August 2020); doi: 10.1117/12.2570725

SPIE.

Event: SPIE Optical Engineering + Applications, 2020, Online Only

Computational Method for Optimizing Segmented Nonimaging Concentrators

Christine Hoffman and Boaz Ilan

Department of Applied Mathematics, School of Natural Sciences, University of California, Merced, California 95344, USA

ABSTRACT

We propose a computational optimization method for designing segmented nonimaging concentrators with planar or tubular absorbers. Concentrators are represented as concatenated linear segments, forming a faceted reflector. Ray tracing is then employed to compute the optical concentration ratio equivalent for a given concentrator configuration. The user may choose to systematically optimize the locations of the concentrator vertices or the interior angles between adjacent segments. Since gradient-based solvers become easily trapped in local minima for this problem, generalized pattern search is used to obtain optimized concentrator configurations. For a small and fixed number of segments, we show that optimized segmented concentrators perform better than an equivalent number of uniformly spaced segments of the collocated ideal shape. We also show that concentrators with a lower number of segments are more robust to manufacturing errors.

Keywords: Nonimaging Concentrators, Solar Concentrators, Optimization, Nonimaging Optics, Ray Tracing

1. INTRODUCTION

Nonimaging optics is an emerging field that rose in prominence in the 1960's with the discovery of compound parabolic concentrators (CPC).¹ Nonimaging solar concentrators have the advantage of being non-tracking solar devices, meaning that no moving mechanical device is needed. As their name suggests, nonimaging concentrators do not necessarily form an optical image of the source, but rather instead aim to maximize all forms of solar light radiation, beam or diffuse, onto the receiver.²

In 2D, one can obtain ideal concentrators using Hottel's strings. However, the 3D designs that result from extending these 2D designs into 3D are not ideal. Furthermore, the reflector shapes are curved. Current production of nonimaging solar thermal reflectors includes precise bending of a reflective material, typically metal sheets. The sheet must not only be continually bent, but also retain their configuration. This increases the manufacturing costs. A cheaper alternative is to bend a flat metal sheet along straight edges, creating what is often called a faceted, or segmented reflector.

CECs, or compound elliptical concentrators, are closely related to CPCs. CPCs have a source at infinity, whereas CECs have a source at a finite distance. CECs are considered ideal in the sense that all rays entering the aperture are collected onto the receiver.

Ideal two dimensional solar thermal concentrators are designed using the method of strings, which utilizes principles from Hottel's strings and the edge ray principle. Hottel's strings were originally used to calculate radiation transfer between walls in a furnace.³ The edge ray principle, based on Hamiltonian and Lagrangian optics, states that redirecting all light rays emanating from the edges of the source towards the edges of the receiver will ensure that all the light rays from the interior of the source will also land on the receiver.

An example of an ideal 2D compound elliptical concentrator (CEC) setup is shown in Figure 1. The linear source, shown on the left in red, and linear receiver, shown on the right in blue, must first be defined. A CEC is uniquely defined for any given extended linear source and linear receiver. Every point on the source is assumed to radiate isotropically. Cross strings $\overline{AC'}$ and $\overline{A'C}$ are drawn from the bottom of the source to the top of the receiver and from the top of the source to the bottom of the receiver, respectively.

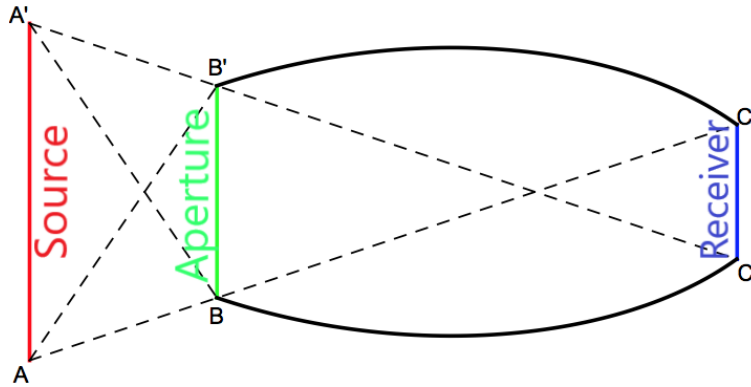


Figure 1. Diagram of an ideal 2D compound elliptical concentrator.

2. FACETED DESIGNS

Segmented nonimaging solar thermal concentrator designs differ from the smooth ideal CPC design in that the troughs are not a smooth curved surface, but rather consist of flat surfaces joined at the edges. Such designs are also known as faceted concentrators. In this way, concentrators may be produced from a single flat reflective piece of metal that is kinked at the various joints to the desired angle between adjacent flat segments.

Reflective metal sheets are more easily kinked at joints to form hinges rather than bent continuously into a smooth curve, reducing production costs. One company, Arctic Solar, uses segmented nonimaging solar thermal concentrator trough designs such as that shown in Figure 2.

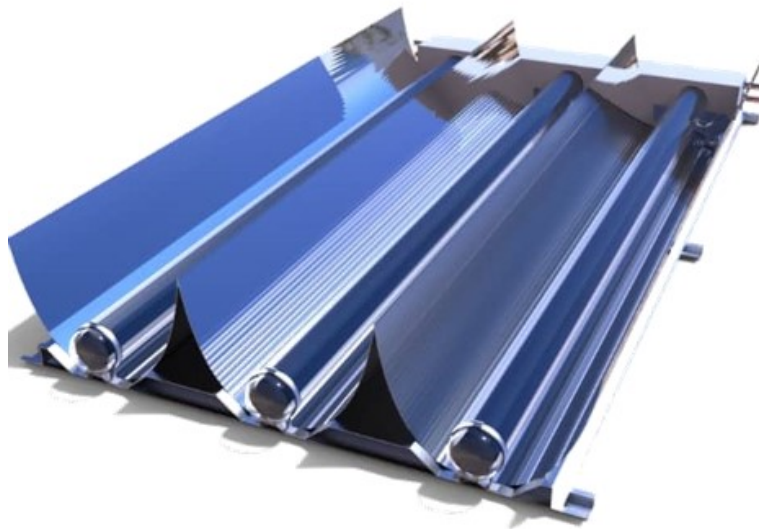


Figure 2. Commercial segmented solar concentrator produced by Arctic Solar, Inc. <http://articsolar.com/>

Despite the possible reduction in manufacturing costs, alternative designs to the ideal nonimaging 2D compound parabolic concentrator (CPC) trough design also face a drawback; they are less than ideal. Less than ideal configurations do suffer from some efficiency loss. Furthermore there is no analytical method to

optimize faceted designs. We therefore turn to computational methods, such as ray tracing, to study design efficiencies.

3. SEGMENTED CONCENTRATOR SETUP

The goal of this paper is to compare the efficiency of segmented solar thermal concentrators with optimally placed joints versus segmented solar concentrators with an equivalent number of joints placed taken from the discretized CPC configuration. All joints are connected to one another by flat concentrator segments, such as that shown in Figure 3. To measure and optimize the efficiency of various segmented solar concentrator configurations, we implemented a vectorized ray tracer combined with pattern search optimization to find new optimal concentrator designs.

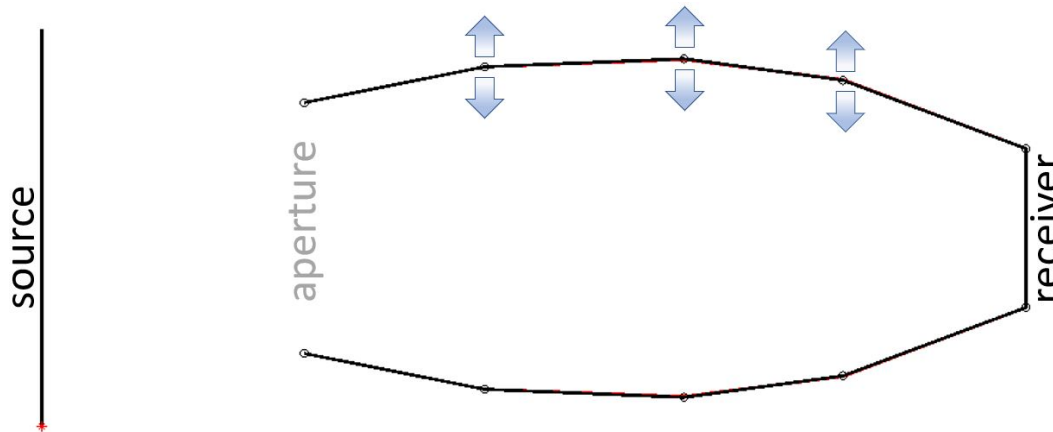


Figure 3. Basic concentrator setup with linear source on left and linear collocated concentrator segments on the right. The linear receiver, aperture, and source are all considered to be fixed. The interior vertices are allowed to move vertically up and down until an optimal concentrator configuration is found.

A source on the left sends rays into the aperture, or opening of the concentrator. The rays then reflect off of the linear collocated concentrator segments until they are either rejected back out through the aperture or reach the receiver. The source, aperture, and receiver are all considered fixed. Hence the vertices on each size of the aperture and the receiver are considered fixed as well.

The other interior vertices are free to move into a configuration that maximizes the percent of rays reaching the receiver from the source. The vertices may move only vertically, as shown by the arrows in the basic concentrator setup of Figure 3, or vertex location may be allowed to move both vertically and horizontally, depending on user preference. Vertically and horizontally moving vertices is one configuration variation of the basic concentrator setup, which only permits vertical variation.

Allowing more flexibility of vertex movements increases the number of degrees of freedom in the optimizer and hence increases optimization difficulty. The process of optimizing the location of these vertices will be discussed in the next chapter.

3.1 Increasing Vertices

With the basic concentrator setup selected, the number of concentrator vertices can be gradually increased incrementally. When a large number of vertices is given to the optimizer, the initial placement of the vertices heavily influences the final optimal configuration found. The heavy influence of the prior placement of the vertices to the final optimal location found means that the initial vertex placement fed into the optimizer should not be arbitrary, but should be rather good, although not optimal.

One way to ensure that the initial placement of vertices fed into the optimizer is not vastly far away from concentrator configurations of high efficiency is to start with a low number of vertices which can be more easily optimized with less influence of the prior and incrementally increase the number of vertices after an optimal configuration is found at each stage. We will describe the process starting with three vertices, or meaning just one interior vertex is optimized.

The y coordinate placement of the single interior vertex is initially optimized. The x coordinate is placed equidistant between the x coordinate of that of the aperture and receiver vertices. The number of interior vertices is then increased by creating a Piecewise Cubic Hermite Interpolating Polynomial, defined as `pchip` in Matlab, through the initial three vertices and placing two interior vertices whose x coordinates are equally spaced between the x coordinates of the aperture and receiver vertices. Therefore the total number of vertices on each concentrator wing is increased to four with one on the aperture, two interior vertices, and one on the receiver.

The concentrator with two interior y vertices placed along the interpolated Piecewise Cubic Hermite Interpolating Polynomial is then optimized. Again, a Piecewise Cubic Hermite Interpolating Polynomial can be used to find the location of three interior y vertices with x coordinate placement equally spaced between the aperture and receiver x coordinate vertex locations. These interpolant vertex locations may be used as the initial vertex placement for the next optimization iteration. This process continues until the desired number of vertices is reached and ensures that initial vertex configurations are not vastly far away from efficient configurations.

3.2 Interior Angle Optimization

Instead of optimizing vertex locations and allowing concentrator segment lengths to vary, such as in the basic concentrator design given in Figure 3, an alternative concentrator configuration is to fix individual concentrator segment lengths and optimize the interior angle between adjacent segments, such as is shown in Figure 4. In this configuration the aperture is not considered fixed and becomes wider or narrower depending on the optimized interior angles.

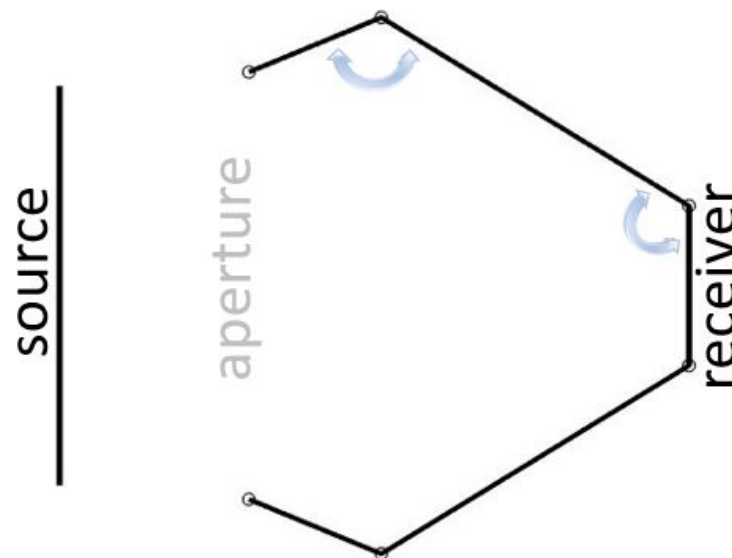


Figure 4. Basic concentrator variation with linear source on left and linear collocated concentrator segments on the right. The linear receiver and source are considered to be fixed. The interior angles are allowed to move until an optimal concentrator configuration is found.

3.3 Trough Concentrator Configuration

The interior angle optimization can be combined with either a flat absorber, as is shown in Figure 4, or a circular absorber, such as is shown in Figure 5. The linear absorber is conformed into a circular segmented absorber along with several concentrator segments along an approximate involute.

This configuration is particularly useful for trough concentrator designs whose absorber has a flowing material, such as oil or sand, encompassed within a vacuum tube. Tubular absorbers are the most commonly deployed design in practice.

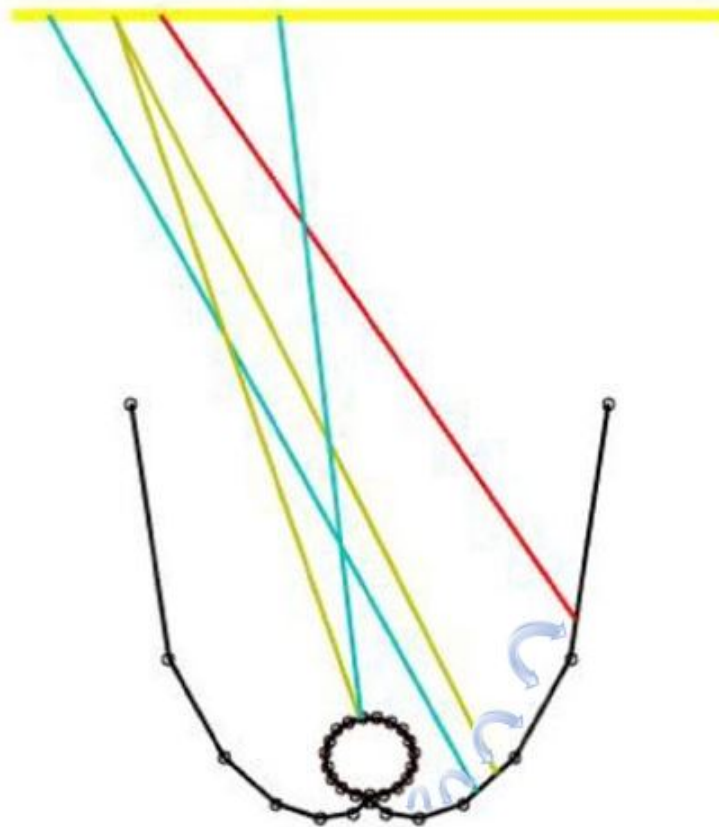


Figure 5. Basic concentrator variation with linear source above and trough collocated concentrator below with circular receiver. The circular receiver and linear source are considered to be fixed. The interior angles are allowed to move until an optimal concentrator configuration is found.

4. OBJECTIVE FUNCTION

The objective is to place the movable vertices in positions that maximize the number of rays hitting the receiver out of those which enter the aperture. However, most optimization methods seek to minimize, not maximize, the objective function. Hence we turn this maximization problem into a minimization problem by minimizing the additive inverse of the optical concentration ratio, meaning our objective function to minimize becomes,

$$F(\mathbf{x}) = -\frac{(\text{number of rays collected on the receiver})}{(\text{total number of rays entering concentrator})} \quad (1)$$

where the vector $\mathbf{x} = (x_1, x_2, x_3, \dots, x_m)$ contains the coordinate points of the vertices of the top polygonal reflector. We enforce symmetry, meaning that the points of the vertices on the lower polygonal reflector are given by $\mathbf{x} = (-x_1, -x_2, -x_3, \dots, -x_m)$.

We also implement constraints which enforce convexity. Without such constraints, we found that the optimizer sometimes becomes stuck in non-convex designs. We only consider convex designs to be practical and therefore implement a convexity constraint.

The total number of rays entering the concentrator is proportional to the incoming radiation flux. The proportional flux is what is measured on the absorber. The numerator of equation (1) is the flux of radiation entering the aperture and the denominator is the flux of radiation incident on the absorber. Hence the ratio of the collected flux on the absorber over the total flux entering the concentrator is maximized.

For an ideal concentrator, $F(\mathbf{x}) = -1$, meaning that all of the rays entering the solar thermal concentrator are collected at the receiver. Since the ideal concentrator is a smooth continuous curve, the discretized linear segmented solar thermal concentrator objective function $F(\mathbf{x})$ will only approach -1 as the number of polygonal reflector vertices (i.e. length of \mathbf{x}) tends to infinity.

We are primarily interested in segmented solar thermal concentrators with low numbers of segments on each wing. In this case we are far from configurations that closely represent the ideal concentrator. Hence the ideal configuration may not be vertices placed exactly along the ideal concentrator.

5. FAILURE OF GRADIENT BASED METHODS

We find that gradient based optimization does not work well, and instead turned to derivative-free optimization techniques. To understand the nature of the objective function given in equation (1) and visually see the reasons gradient based solvers fail, we investigated the nature of the objective function for a single interior movable vertex as shown in Figure 6. The vertices on either side of the aperture and receiver remain fixed while the y -coordinate of a single interior vertex is allowed to vary between the values of 1 to 6. The interior vertex has a fixed x -coordinate midway between the x -coordinates of the aperture and receiver.

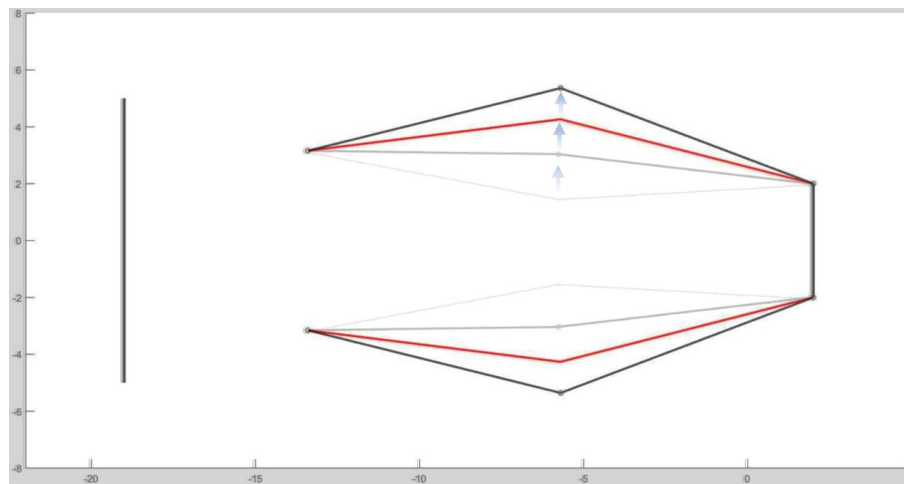


Figure 6. The above figure shows how the y -coordinate of a single joint is changed between the values of 1 to 6.

As the y -coordinate was varied between 10,000 evenly spaced values between 1 and 6, the optical concentration ratio, or additive inverse of equation (1), of each concentrator configuration was recorded. The resulting graph of the negative objective function versus the y -coordinate of the single moving vertex is shown in Figure 7.

The y -coordinate values corresponding to a linear concentrator is denoted by a green circle and the y -coordinate position of the vertex lying on the ideal concentrator is denoted by a red circle in Figure 7.

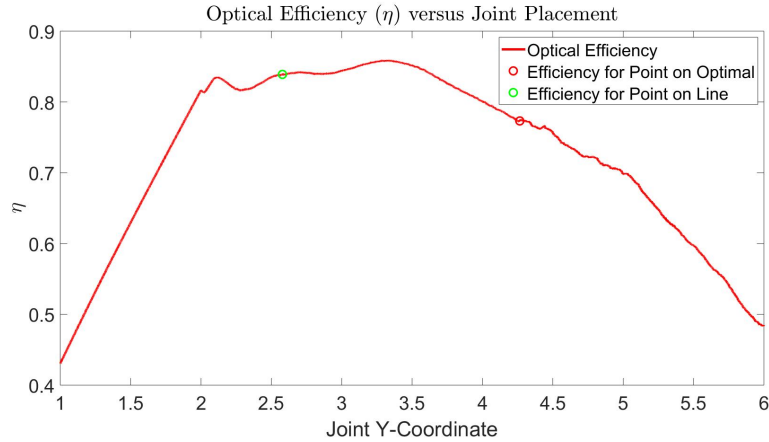


Figure 7. The above graph shows how the optical efficiency changes with the y -coordinate location of a single joint. Notice that neither the location of the y -coordinate corresponding to that of a linear receiver, nor that with the y -coordinate placed at the location along the ideal concentrator result in maximum optical efficiency. Furthermore, the graph has several local maxima/minima, making gradient based methods ineffective at finding the maximum.

Neither one of these gives a configuration that maximizes the percentage of rays reaching the receiver, but rather some intermediate y value between these two configurations. Several local minima and maxima can be observed but overall the graph *appears* quite smooth in areas, such as around the green open circle denoting the location of the linear concentrator.

However, when zooming into Figure 7 in the seeming flat area around green circle of the linear concentrator, we see that the graph no longer looks smooth and several local minima and maxima become apparent, as shown in Figure 8. The graph is indeed locally flat almost everywhere, with abrupt jumps in optical efficiency. This perspective demonstrates the plethora of local minima and maxima at the fine mesh scale. The fractal like nature of local minima and maxima at various scale levels, combined with the locally flat everywhere nature of the objective function make derivative-based solvers unsuccessful. The fractal like behavior of local minima and maxima at different scales is also shown when increasing the dimensions of the problem.

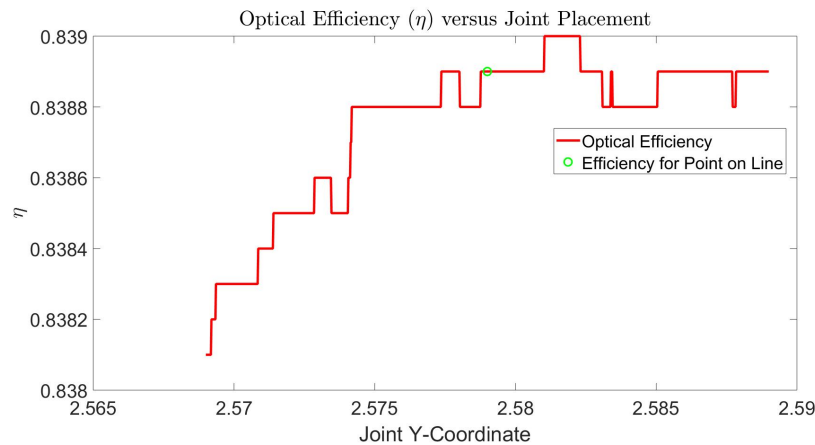


Figure 8. With a mesh of 0.00002 around the location of the y -coordinate for a linear concentrator, we see that the objective function is locally very flat, with sudden jumps in optical efficiency.

6. OPTIMIZATION VALIDATION

We allowed both the x and y coordinates of the single vertex to vary as shown in Figure 9, and plotted the efficiency of the concentrator design corresponding to each vertex placement in the contour plot of Figure 10.

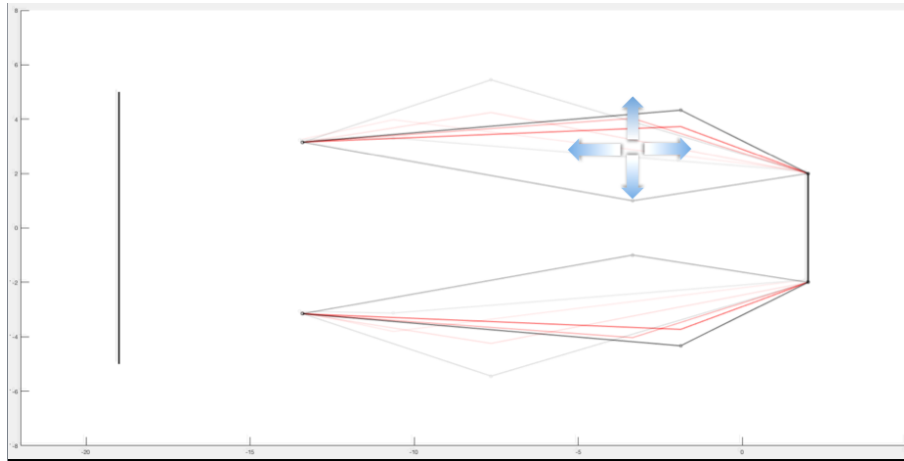


Figure 9. This figure shows how the coordinates of a single vertex can be varied in both the x and y directions.

Again, note that the optimal location for the placement of a single vertex is at an intermediate point between a linear concentrator and a single vertex located on the ideal concentrator, since the optimal appears between the green and red curves on the graph of Figure 10. This indicates the need for the optimized placement of vertices for low degree linear segmented solar thermal concentrators since the optimal y -coordinate placement is not along that for ideal concentrator nor is the optimal x -coordinate equidistant between aperture and receiver.

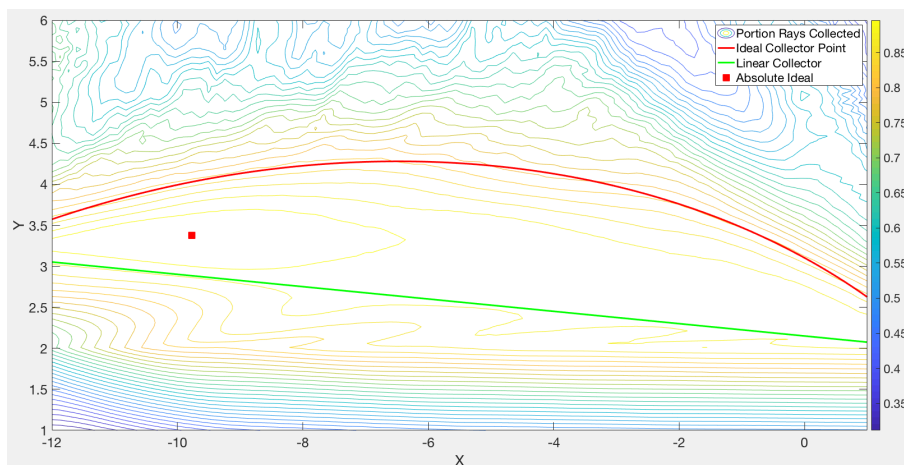


Figure 10. Contour plot showing the percentage of rays collected for a single vertex placed at given x and y coordinates.

When we allowed pattern search to optimize the location of a single vertex for a linear segmented solar concentrator of two segments, such as that in Figure 9, the optimized concentrator was found to be that shown in red of Figure 11.

The configuration and efficiency obtained by the pattern search optimized concentrator is confirmed by the vertex location of highest efficiency found in Figure 10. This result validates that pattern search is working as expected and is able to find the optimal concentrator configurations.

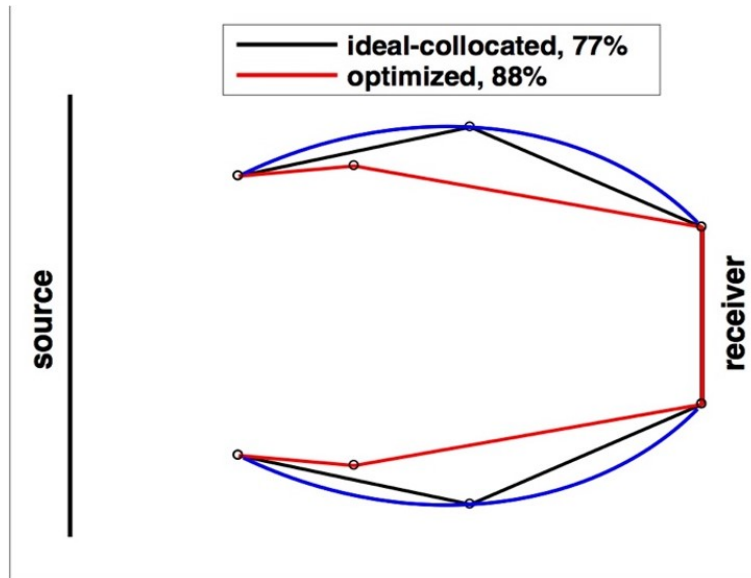


Figure 11. Efficiency Gain for Optimized Segmented Solar Concentrator

7. SMALL NUMBER OF SEGMENTS ADVANTAGE

Figure 11 also shows the real advantage of optimized segmented solar concentrators is when there are just a few number of segments whose location is optimized. When a joint is simply chosen along the ideal equidistant from the aperture and receiver, as shown by the ideal-collocated configuration, such a concentrator configuration only performs at 77% efficiency. On the other hand, the optimized concentrator boasts an efficiency of 88%, an 11% efficiency gain.

The (x, y) vertex position of the two linear segmented optimized concentrator in Figure 11 is similar to the optimal vertex location found in Figure 10. Optimized segmented solar thermal concentrators show the most efficiency gain over their ideal-collocated counterparts when there are fewer segments.

When the number of segments is large, we see that the segmented solar thermal concentrator often approaches the shape of the ideal solar thermal concentrator with increasing efficiency. As the number of segments increases, the added increase from the optimization process becomes less significant. Hence, ideal-collocated and optimized segmented solar concentrators composed of a high number of linear segments on each wing do not show significant efficiency differences.

To display the optimization advantage, Figure 12 shows the difference in efficiency for an optimized concentrator of the specified number of segments versus a collocated ideal concentrator with an equivalent number of vertices. The plot was produced starting with a basic concentrator setup, such as that in Figure 3, optimizing a single interior vertex.

There were a total of three vertices along each of the top and bottom concentrator wings corresponding to one on the aperture, an interior vertex, and on the receiver. The x value of the interior vertex was fixed half way between the x coordinate values of the aperture and receiver vertex values.

The respective optimized and ideal collocated segmented concentrators are shown on the right. The efficiencies of each concentrator relative to the number of segments is shown on the left. The largest different between the two curves in Figure 12 is for low numbers of segments with the greatest different being for a concentrator consisting of just two segments.

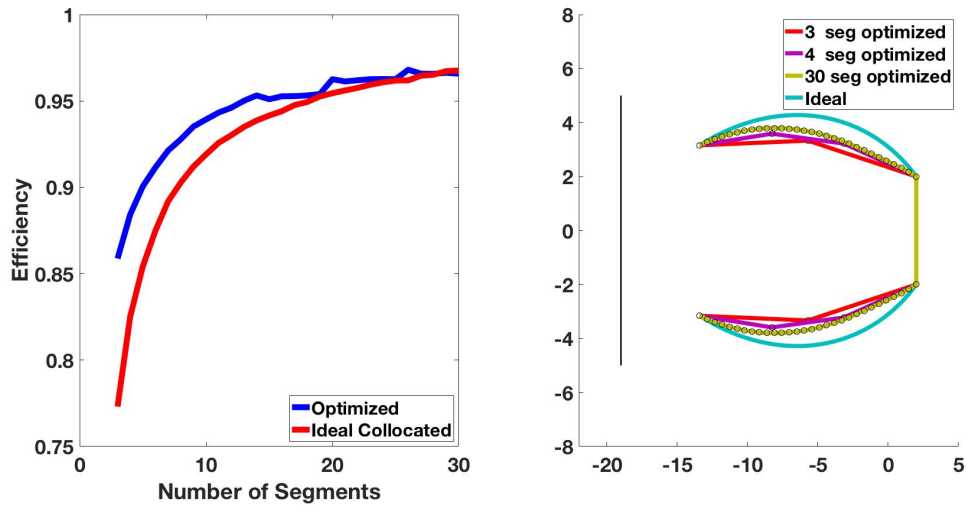


Figure 12. As the number of segments increases, the efficiency of the ideal-collocated segmented concentrator approximately equals the efficiency of an optimized segmented collocated linear concentrator. However, the optimized concentrators show much higher efficiency for low numbers of segments.

8. SENSITIVITY ANALYSIS

Assessing the sensitivity of various concentrator configurations is very important to predict the performance of manufactured concentrators. Some analytical work has been done looking at the error in the concentrator slopes and its effect on acceptance angles.¹ It is thought that nonimaging designs are more robust to manufacturing errors.

We take a computational approach instead of an analytical approach and directly quantify efficiency losses with respect to manufacturing errors. We provide a systematic assessment of concentrator sensitivity under various degrees of manufacturing errors. This approach and level of theoretical sensitivity assessment which quantifies manufacturing error effects on device performance has not been done previously.

8.1 Sources of Concentrator Defects

In practice, concentrator segments would be manufactured and cut to specified lengths. However, there is inherent error in cutting and connecting concentrator segments. Segment length error would inevitably lead to a decrease in efficiency.

The degree to which error is tolerated depends partly on the number of segments the concentrator has. Clearly a concentrator with many segments, meaning many shorter segments, will require a machine with lower tolerance. Concentrators with only a few, longer segments can allow a higher error tolerance.

We define noise relative to the length scale of the segments by the following equation:

$$y_{\text{noise}} = (\text{length scale}) \times (\text{random normal}[0, \text{noise deviation}]) \quad (2)$$

where

$$(\text{length scale}) = \frac{(x_{\text{receiver top}} - x_{\text{aperture top}})}{(\text{number of segments on concentrator})} \quad (3)$$

and the noise deviation varies from 0 to .05 in .01 increments.

In Figure 13, we see that concentrator efficiency decreases with increasing levels of noise, as we would expect. However, there are particularly large drops in efficiency for concentrators with a large number of segments.

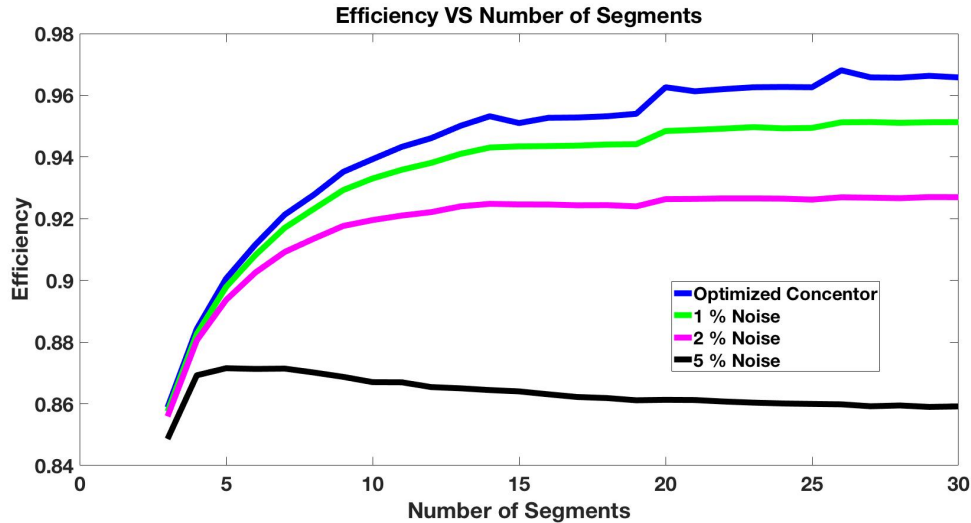


Figure 13. Inherent manufacturing errors lead to decreased efficiencies. The above figure shows how errors, modeled through adding noise to joint placement, compromise efficiency. Concentrators with large numbers of segments, and hence have a large number of joints, are more prone to large efficiency drops with too much noise since errors occur at each of the joint locations.

The reason the amount of error plays a larger role in efficiency for a large number of segments is likely due to the fact that error in each segment is contributing to the drop in performance. Concentrators with fewer segments have fewer sources of error to occur, even if deviation from the optimized location is larger.

Low degree concentrators are the most robust to noise errors. We see that the difference in performance for really low degree concentrators does not change much even when adding as much as 5% noise.

However, as the number of segments increases, noise levels become more important. Concentrators with a large number of segments, but also lots of noise show little to no improvement over concentrators with fewer numbers of segments. This is especially true for noise above 2%, after which device performance can actually decrease when adding more segments, such as is the case for 5% noise.

9. SPEED ASSESSMENT

The ray tracer is vectorized in Matlab and optimization is highly efficient when paired with Matlab's built in pattern search optimization function. No communication between various platforms is needed, increasing speed.

The output in Table 1 shows only 0.034882 seconds and 3 complete iterations and are needed to achieve a mesh tolerance of less than 10^{-8} when optimizing the y coordinate of a single vertex of the basic concentrator. Even when vertices are increased, pattern search still only requires seconds to optimize even 28 interior vertices.

Typically less than 7 iterations are required by pattern search to reach an optimum within a tolerance of 10^{-8} within a run time of seconds. The mesh size decreases approximately by a power of 10 with each displayed iteration. Since we have a nonlinear constrained problem, the method column either displays 'Increase penalty', or 'Update multipliers', which refers to changes implemented on the Lagrangian multipliers by the pattern search optimizer.

The maximum constraint column displays a positive value of 0.5 if the constraints are not satisfied and 0 if the constraints are satisfied. The constraint is initially not satisfied since the initial vertex lies on a linear concentrator wing, which is not convex. The column $f(x)$ refers to the value of the objective function.

Iter	Func-count	f(x)	Max Constraint	MeshSize	Method
0	1	-0.8389	0.5	0.1	
1	7	-0.857	0	0.001	Increase penalty
2	29	-0.8582	0	9.333e-07	Update multipliers
3	71	-0.8588	0	8.71e-10	Update multipliers

Optimization terminated: mesh size less than options.MeshTolerance
and constraint violation is less than options.ConstraintTolerance.
Elapsed time is 0.030852 seconds.

Table 1. The above display shows the Matlab console output when optimizing the y coordinate of a single vertex of the basic concentrator.

10. ACHIEVEMENTS AND RESULTS OF METHOD

Although ideal 2D CEC designs exist, the performance of these designs quickly changes when the concentrator is approximated by segmented collocated linear segments. We aim to remove the limitations of continuously varying shapes and 2D designs by taking a computational approach.

Our computational approach includes optimizing segmented solar concentrator efficiency for a given number of segments. The result is a design that is relatively easy to manufacture, while maximizing efficiency for the given design constraints. Our computation methods achieved the following goals:

- Easy to manufacture
- Adaptable to different user designed configuration criteria and constraints
- Highly efficient, optimal, and practical
- Computationally fast
- Robust to slight changes caused by error

Our method addresses all of these goals. In addition, our method can be used to design low degree efficient concentrator designs which have not been discussed in other literature.

10.1 Easy to Manufacture

One primary goal achieved was designing a concentrator that can be manufactured cheaper while minimally sacrificing concentrator efficiency. We call such concentrators to be optimal. They are no longer ideal in terms of collecting every ray that enters the aperture, they give the highest optical concentration ratio efficiency for the given design parameters.

There are several factors which make may make linear segmented concentrators easier and cheaper to manufacture, which include:

- Linear segments instead of curved surfaces
- Efficient low degree concentrators
- Symmetric
- Definable concentrator wing lengths
- Definable aperture size
- Definable absorber shape

10.2 Optimized by a computationally fast approach

We have shown that our method gives theoretically efficient designs and results in practical configurations in seconds. Our vectorized ray tracing method in Matlab combined with Matlab's built in pattern search optimization give results in seconds. If one were to use multiple softwares for the ray tracing and optimization, there would be a huge communication lag between various softwares. We implement everything in Matlab and our method is also not proprietary.

Our optimizer allows the user the adaptability to choose the number of vertices while optimizing at each step. The number of vertices is increased incrementally, optimizing at each step, until the desired number of vertices is reached. The optimizer used to determine the optimal concentrator configuration is fast and also gives good results. This is made possible by using:

- Vectorized ray tracer
- Single software for both ray tracer and optimizer to reduce communication lag between various softwares
- Any number of segments on reflector

10.3 Adaptable to Various Design Criteria

Our method also allows lots of user flexibility to specify design criteria. Some user specified parameters include the number of segments, optimization preferences such as interior angle or vertex location optimization, and ray configuration. Hence, users can optimize a configuration that fits their needs.

Users may also choose trough or basic concentrator configurations. These two configurations optimize different aspects of the concentrator configuration: joint coordinate values or interior angles between consecutive segments. Optimizing the angles between consecutive segments while keeping segment lengths fixed seems to be a more realistic portrayal of the manufacturing process. However, optimizing interior angles moves the location of the aperture.

Setups which require specific aperture sizes or the ability to increase the number of segments may prefer joint coordinate optimization. Configurations with larger numbers of segments were also less dependent on the initial configuration if segments were incrementally increased with coordinate joint locations were optimized at each step. Both approaches lead to comparably efficient designs overall.

Therefore, we addressed the fact that concentrator designs are adaptable to various design parameters such as:

- Any absorber shape
- Fixed wing lengths or maximum concentrator width/length
- Maximum or fixed aperture size

10.4 Robust to manufacturing errors

The new low degree designs that we were able to find with our optimization method displayed:

- Robust to slight changes, especially for low segmented designs
- Limited efficiency losses from small design errors
- For concentrators with up to 5 segments, low efficiency losses, even with higher amounts of error
- Limited efficiency loss due to inherent manufacturing errors

10.5 Highly efficient, Optimal, and Practical

We were also able to show that pattern search is able to find the most optimal configuration when optimizing over two degrees of freedom. Our method is also able to effectively find optimal designs, with concentrator efficiency above segmented ideal concentrators. We also enforce convexity, preventing the optimizer from becoming stuck in impractical, nonconvex configurations.

Optimized low segmented designs are also shown to result in the highest efficiency gains compared to a segmented concentrator of collocated points along the ideal. Therefore, we were able to show that our method results in:

- Optimized concentrator configurations under given constraints
- At least or more efficient designs compared to collocated segmented ideal concentrators
- Optimized low segmented designs show the highest efficiency gains compared to collocated points along the ideal
- Convexity can be enforced on the reflector shape

Overall, we showed that our method is not only fast, but is shown to be effective in finding optimal designs specifically for low degree optimization problems. This is important since these configurations are of most interest in terms of manufacturing, robustness, and efficiency gains.

REFERENCES

- [1] Winston, R., W. T. Welford, J., Minano, J., Benitez, P., Bortz, W., (Firm), K., Shatz, N., and Bortz, J., [*Nonimaging Optics*], Electronics & Electrical, Elsevier Science (2005).
- [2] Duffie, J. and Beckman, W., [*Solar Engineering of Thermal Processes*], Ingenieria de la Energia, Wiley (2013).
- [3] Winston, R., Jiang, L., and Ricketts, M., "Nonimaging optics: a tutorial," *Adv. Opt. Photon.* **10**, 484–511 (Jun 2018).